Transactions on Environment, Energy and Earth Sciences
ISSN: 2960-1924, eISSN: 2960-2300 | Volume 2
ERET 2024

Combining Machine Learning and Remote Sensing for Online Environmental Quality Monitoring and Cause Analysis in Xiamen, China

Honghui Yang [1], Weizhen Xu [2, *], Zhengyan Chen [1], Jiao Yu [2]

[1] Fujian Agriculture and Forestry University, Fuzhou, China

[2] Tongji University, Shanghai, China

* Corresponding Author Email: fjxwz@tongji.edu.cn

Abstract. This study focuses on Xiamen, China, and uses the Google Earth Engine (GEE) platform to calculate the city's Remote Sensing Ecological Index (RSEI) from 2000 to 2020, analyzing the temporal and spatial changes in environmental quality. Additionally, it integrates the eXtreme Gradient Boosting (XGBoost) model and SHapley Additive exPlanations (SHAP) algorithms to analyze the driving factors affecting changes in the environmental quality of Xiamen. The results of the study show that: (1) From 2000 to 2020, the environmental quality in Xiamen City showed a trend of "first increase and then decrease", with the average value of RSEI increasing from 0.55 to 0.57 and then slightly decreasing to 0.56. (2) During 2000 to 2020, the majority of Xiamen's environment quality improved, covering 44.75% of the area. However, regions where the environment deteriorated were primarily located along the coast in Jimei district and Xiang'an district, accounting for 32.58% of the total area. (3) Elevation, slope, percentage of construction area, annual average precipitation, and percentage of cropland area are the five factors with the greatest impact on environmental quality. The effects of elevation and slope on environmental quality exhibit a quadratic function relationship, while percentage of construction area, annual average precipitation, and percentage of cropland area show linear relationships.

Keywords: Machine learning; remote sensing; environmental monitoring; RSEI; SHAP.

1. Introduction

Scientific and accurate monitoring of regional environmental quality, along with further analysis of its temporal and spatial evolution and influencing factors, is crucial for advancing ecological civilization and promoting sustainable development. With the rapid development of remote sensing technology, many scholars have applied it to the assessment and monitoring of environmental quality. For instance, indicators such as the Normalized Difference Vegetation Index (NDVI) [1], land cover types [2], Land Surface Temperature (LST) [3], and the Normalized Difference Water Index (NDWI) [4] are used for environmental quality assessments. However, due to the complexity and diversity of ecosystems, a single indicator often fails to comprehensively reflect the environmental quality under the influence of multiple factors [5]. Therefore, some studies have conducted environmental quality assessments by integrating multiple indicators, utilizing methods such as the Pressure-State-Response (PSR) model [6, 7], and the Ecological Index (EI) [8] to evaluate the health of ecological environment. However, the difficulty in obtaining statistical data for certain regions, coupled with the influence of subjective factors on the weighting of indicators within models, makes it challenging to accurately reflect the temporal and spatial changes in environmental quality [9]. To address this, Hanqiu Xu developed the Remote Sensing Ecological Index (RSEI) by integrating four indicators: greenness (NDVI), moisture (WET), heat (LST), and dryness (NDBSI). Principal Component Analysis (PCA) was then used to assign weights to these factors. Compared to traditional methods of environmental quality assessment, RSEI offers a more objective and efficient means of capturing changes in environmental quality and boasts advantages such as data visualization and high precision [10]. It has been widely applied to environmental quality monitoring in various regions including urban clusters [11, 12], plateaus [13], and river basins [14]. However, long-term monitoring studies focused on the

environmental quality of bay cities are still relatively scarce, and further research into their driving factors is needed.

In analyzing the causes of regional environmental quality changes, many studies use methods such as Geodetector [15], Geographically Weighted Regression (GWR) [16], and Multiscale Geographic Weighted Regression (MGWR) [17] to investigate the main drivers of environmental quality changes. With the development of machine learning in recent years, an increasing number of researchers are using methods like Gradient Boosting Decision Tree (GBDT) [18], eXtreme Gradient Boosting (XGBoost) model [19], and Random Forest algorithm [20] to explore the correlations between environmental quality and multiple variables. Among these, the XGBoost model, as an enhancement of the GBDT model, reduces the risk of overfitting in machine learning models by incorporating regularization terms. It shows significant improvements in algorithm execution speed and the precision of loss function calculations [21]. However, despite the XGBoost model's significant advantages in terms of fit and prediction accuracy, its interpretability regarding the interactions among variables within the model still requires further investigation. SHapley Additive exPlanations (SHAP), a machine learning explanation tool based on game theory, addresses this by using the Monte Carlo sampling method to calculate the SHAP values for each variable. This tool offers strong global and local interpretability of variables, fair distribution of variable contributions, and visual representation of results. These features help overcome the limitations of the XGBoost model's poor interpretability [22, 23], facilitating a deeper exploration of the interactions between regional environmental quality changes and various factors.

Xiamen, located in the southeastern part of Fujian Province, China, is a bay city (see Fig. 1) situated in a special area where land and sea interact. Compared to inland cities, its ecosystem is more sensitive. Since the reform and opening-up policy, the expansion of construction land within Xiamen has been rapid, and ecological security issues have become increasingly severe, making it a typical example of ecological vulnerability in coastal cities [24]. Therefore, monitoring the environmental conditions of Xiamen and analyzing their causes are crucial for advancing the city's ecological urban development and achieving high-quality social development. Based on this context, this study focuses on Xiamen City, utilizing the Google Earth Engine (GEE) platform to construct RSEI to analyze the environmental quality changes in 2000, 2010, and 2020. Furthermore, the XGBoost algorithm is selected to build a machine learning model, combined with SHAP to calculate and analyze the mechanisms through which various variables affect the RSEI. This approach aims to provide a scientific basis for urban planning efforts and offer references for ecological urban development in other coastal regions.

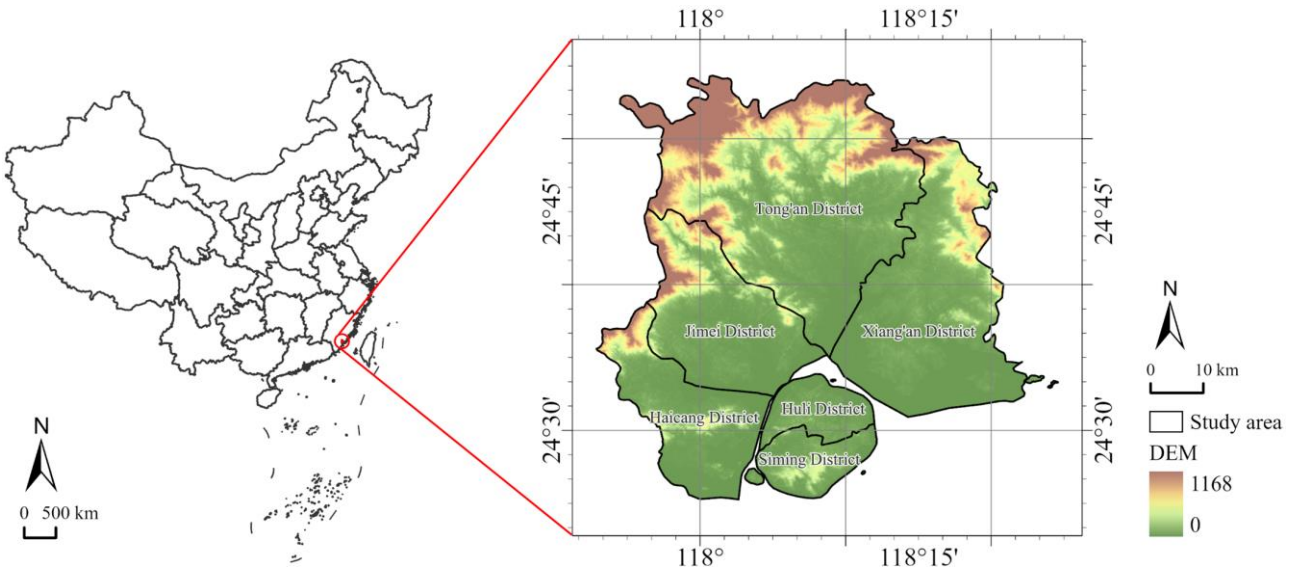

Figure 1. Geographical location of Xiamen

2. Data and Methodology

2.1. Data Sources and Preprocessing

This study utilizes Landsat TM/OLI remote sensing imagery from the years 2000, 2010, and 2020, accessed through the Google Earth Engine (GEE) platform, which has already undergone geometric, radiometric, and atmospheric corrections. Additionally, the Landsat cloud masking algorithm available on the GEE platform is used to detect and remove cloud pixels and shadows from the imagery. Images from the same year that are cloud-free (from March to September) are used to fill in gaps, thus ensuring that only the highest quality remote sensing images are selected for the study area. Finally, a total of 46 satellite images were mosaicked to form composite images of Xiamen City for the three periods with minimal cloud cover, each with a spatial resolution of 30 m. Additionally, to avoid the influence of large water bodies on the principal component load distribution, this study utilized the Modified Normalized Difference Water Index (MNDWI) to mask water body information, ensuring that the wetness indicator accurately represents the moisture conditions of the study area.

Land use type data were obtained from the China Land Cover Dataset (CLCD) [25], which has a spatial resolution of 30 m and an overall accuracy of 79.31%, suitable for research purposes. Subsequently, the data were cropped and reclassified into five categories in ArcGIS: cropland, forest, grassland, water, and construction land. The Digital Elevation Model (DEM) was sourced from the Geospatial Data Cloud (http://www.gscloud.cn/) and processed in ArcGIS to derive the slope of the study area. Additionally, the study included data on annual average rainfall, annual average temperature, population density, and Gross Domestic Product (GDP). Specific sources and preprocessing steps for these data are detailed in Table 1.

Table 1. Data Source and Pre-processing

Name	Source	Time	Resolution	Pre-processing
Annual average rainfall	http://loess.geodata.cn/	2020	1 km	Image cropping
Annual average temperature	http://loess.geodata.cn/	2020	1 km	Image cropping
Population density	https://www.worldpop.org/	2020	1 km	Image cropping
GDP	https://www.resdc.cn/	2020	1 km	Image cropping

2.2. Methodology

1) Calculation of RSEI:

Table 2. Calculation Formulae for Each Indicator

Indicators	Calculation methods
NDVI	$NDVI=(\rho_{NIR}-\rho_{red})/(\rho_{NIR}+\rho_{red})$
WET	$WET_{TM}=0.0315\rho_B+0.2021\rho_G+0.3102\rho_R+0.1594\rho_{NIR}-0.6806\rho_{SWIR1}-0.6109\rho_{SWIR2}$ $WET_{OLI}=0.1511\rho_B+0.1973\rho_G+0.3283\rho_R+0.3407\rho_{NIR}-0.7117\rho_{SWIR1}-0.4559\rho_{SWIR2}$
LST	$LST=T/\left[1+\left(\frac{\lambda T}{\rho}\right)\cdot\ln\varepsilon\right]-273.15$
NDBSI	$IBI=\{2\rho_{SWIR1}/(\rho_{SWIR1}+\rho_{NIR})-[\rho_{NIR}/(\rho_{NIR}+\rho_R)+\rho_G/(\rho_G+\rho_{SWIR1})]\}/\{2\rho_{SWIR1}/(\rho_{SWIR1}+\rho_{NIR})+[\rho_{NIR}/(\rho_{NIR}+\rho_R)v\rho_G/(\rho_G+\rho_{SWIR1})]\}$ $SI=\frac{[(\rho_{SWIR1}+\rho_R)-(\rho_B+\rho_{NIR})]}{[(\rho_{SWIR1}v\rho_R)+(\rho_Bv\rho_{NIR})]}$ $NDBSI=(IBI+SI)/2$

NDVI: Normalized difference vegetation index. LST: Land surface temperature. NDBSI: Normalized difference impervious surface index. IBI: Index-based built-up index. SI: Soil index. ρ_{red}, ρ_B, ρ_G, ρ_{NIR}, ρ_{SWIR1}, ρ_{SWIR2} are the reflectance of the red, blue, green, near infrared, short-wavelength infrared 1, and short-wavelength infrared 2 bands of Landsat 5 TM and Landsat 8 OLI, respectively. T: Brightness temperature for conversion of thermal radiation intensity. λ: Thermal infrared central wavelength. $\rho=1.438\times10^{-2}$ mK. ε: Land surface emissivity [5].

RSEI is composed of four indicators: greenness (NDVI), humidity (WET), heat (LST), and dryness (NDBSI), with values ranging between [0, 1]. Values closer to 1 indicate better environmental quality [10]. Wherein, greenness is represented by the Normalized Difference Vegetation Index (NDVI), which is used to reflect the distribution of vegetation density and the condition of plant growth within the region [26]. Humidity is derived from tasseled cap transformations and can reflect the moisture of vegetation and soil [27]. Dryness is calculated using the built-up index (IBI) and soil index (SI) [28]. And heat index is represented by surface temperature, which is obtained through the single window algorithm [29]. The specific formulas for each indicator are shown in Table 2.

It is important to note that since the four indicators have different units and numerical ranges, they each require normalization to standardize their scales, as shown in (1).

$$NI_i=(I_i–I_{min})/(I_{max}–I_{min}) \quad (1)$$

Where NI_i is the normalized indicator value. I_i is the indicator value. I_{max} and I_{min} are the maximum and minimum values of the indicator respectively.

After normalization of each indicator, the initial Remote Sensing Ecological Index ($RSEI_0$) is obtained through Principal Component Analysis (PCA), as shown in (2).

$$RSEI_0=1–\{PC1[f\ (NDVI, Wet, LST, NDSI)]\} \quad (2)$$

Where *PC1* denotes the first principal component and *f* is the normalization of each indicator.

The $RSEI_0$ is normalized to obtain the final RSEI value, as shown in (3).

$$RSEI=(RSEI_0–RSEI_{0\ min})(RSEI_{0\ max}–RSEI_{0\ min}) \quad (3)$$

$RSEI_{0\ max}$ and $RSEI_{0\ min}$ represent the maximum and minimum values of $RSEI_0$, respectively.

2) XGBoost Model and SHAP Method

The XGBoost model is a machine learning algorithm based on Gradient Boosting Decision Tree that can capture nonlinear relationships between variables. This model offers faster computation speeds and higher operational efficiency compared to Random Forest and Support Vector Machine. The SHAP method not only quantifies the contribution and polarity of independent variables to the dependent variable but also provides global and local interpretations of machine learning models [30]. Therefore, this study constructs the XGBoost model using RSEI as the dependent variable and factors such as elevation, slope, annual average rainfall, annual average temperature, population density, and GDP as independent variables. Additionally, the SHAP method is used in conjunction with the XGBoost model to interpret and estimate the contribution rates of each factor to RSEI. The specific principles are shown in (4).

$$g(z') = \emptyset_0 + \sum_{i=1}^{M} \emptyset_i z'_i \quad (4)$$

In the equation, $g(z')$ represents the predicted impact value of the indicator z' on ecological quality, $\emptyset_0$ represents the average value of ecological quality, *M* represents the number of variables in the model, and $\emptyset_i$ represents the SHAP value of the *i*-th indicator [31].

3. Results

3.1. Results of the Principal Component Analysis for Each Indicator

From Table 3, it is evident that: (1) From 2000 to 2020, the first principal component (PC1) contributed more than 70% to the RSEI, with NDVI and WET consistently showing positive values and LST and NDBSI consistently showing negative values. This indicates that greenness and humidity positively influence the environmental quality of Xiamen, which aligns with actual conditions. (2) The signs of the four indicators vary in PC2 to PC4, making it difficult to interpret ecological phenomena consistently. In summary, PC1 not only integrates the characteristic information of the four indicators but also corresponds with reality, making it suitable for constructing the RSEI model for Xiamen.

Table 3. Principal Component Analysis of Each Indicator from 2000 to 2020

Year	Index	PC1	PC2	PC3	PC4
2000	NDVI	0.4788	0.5654	0.4104	0.5317
	WET	0.5032	-0.6970	-0.2226	0.4599
	LST	-0.4717	-0.3952	0.7388	0.2747
	NDBSI	-0.5432	0.1959	-0.4860	0.6560
	Eigenvalue	0.2463	0.0460	0.0147	0.0047
	Percent eigenvalue	79.01%	14.77%	4.72%	1.50%
2010	NDVI	0.5517	0.4964	0.4012	0.5368
	WET	0.4279	-0.8228	-0.0635	0.3686
	LST	-0.4614	-0.2648	0.8420	0.0897
	NDBSI	-0.5474	0.0803	-0.3549	0.7536
	Eigenvalue	0.3121	0.0359	0.0181	0.0028
	Percent eigenvalue	84.62%	9.73%	4.90%	0.75%
2020	NDVI	0.5979	0.3407	0.5151	0.5110
	WET	0.3728	-0.7649	-0.3312	0.4078
	LST	-0.4541	-0.4841	0.7401	0.1082
	NDBSI	-0.5453	0.2539	-0.2780	0.7490
	Eigenvalue	0.2597	0.0210	0.0084	0.0011
	Percent eigenvalue	89.49%	7.22%	2.91%	0.38%

3.2. Analysis of the Temporal and Spatial Changes in Environmental Quality of Xiamen City

To more intuitively reflect the environmental quality in Xiamen, the RSEI values were classified into five categories using the equal interval method in ArcGIS Pro [10]: poor (0-0.2), fair (0.2-0.4), moderate (0.4-0.6), good (0.6-0.8), and excellent (0.8-1). Meanwhile, the area percentages of different environmental quality categories for the three periods were calculated (Table 4) and their spatial distribution was mapped (see Fig. 2). Overall, the environmental quality of Xiamen has not changed much from 2000 to 2020, with the average value of RSEI showing a state of "rising and then falling", from 0.55 to 0.57, and then dropping slightly to 0.56.

Table 4. Statistics of Ecological Quality Grade and Area of Xiamen from 2000 to 2020

Year	2000		2010		2020	
Grade	Area (km²)	Scale (%)	Area (km²)	Scale (%)	Area (km²)	Scale (%)
Poor (0-0.2)	224.74	15.15%	303.99	19.65%	243.93	15.51%
Fair (0.2-0.4)	230.40	15.54%	201.38	13.02%	304.31	19.35%
Moderate (0.4-0.6)	354.23	23.89%	223.69	14.46%	275.17	17.50%
Good (0.6-0.8)	320.96	21.64%	289.79	18.73%	286.20	18.20%
Excellent (0.8-1)	352.66	23.78%	528.18	34.14%	463.23	29.45%
Average of RSEI	0.55		0.57		0.56	

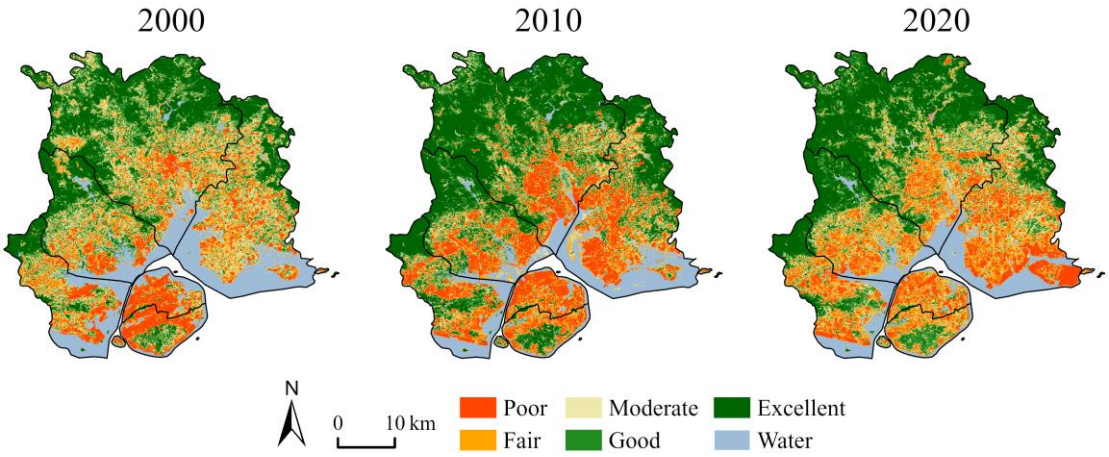

Figure 2. Distribution of RSEI ratings in Xiamen from 2000 to 2020

In terms of spatial characteristics, the spatial pattern of environmental quality in Xiamen exhibited a "low in the south, high in the north" distribution, which aligns with the general topographical features of the area. Development is easier in the low-altitude plain areas, hence areas of significant environmental degradation are primarily located within Xiamen Island and along the coastal areas outside the island. Due to the presence of mid to low mountainous areas along the northern boundaries of Xiamen, which are less conducive to development and socio-economic activities, this region boasts higher vegetation cover and excellent environmental quality. More specifically: (1) From 2000 to 2010, the environmental quality in Xiamen improved, with the area proportion classified as excellent increasing by 10.36%, exceeding 30% of the total area. Areas of poorer environmental quality were primarily concentrated on the island (Huli and Siming districts) and along the coastal areas outside the island. (2) From 2010 to 2020, there was a slight decline in environmental quality in Xiamen, with the total area categorized as moderate and below increasing by 94.36 km², raising the overall percentage to 52.35%. Although the areas categorized as poor decreased during this period, the rapid urbanization process and significant increase in construction land led to a slight overall decline in environmental quality.

Fig. 3 and Tables 5 illustrate the environmental quality changes in Xiamen from 2000 to 2020. Overall, during these 20 years, areas with slight to significant improvements in environmental quality totaled 660.88 km², accounting for 44.75% of the total area. This means that despite the high rate of urbanization in Xiamen, the environmental quality is generally improving due to the government's active ecological management projects and renovation of old urban areas. In detail: (1) From 2000 to 2010, the predominant trend in Xiamen's environmental quality was improvement, with areas showing slight to significant improvements accounting for 47.66% of the total study area, while areas where environmental quality deteriorated made up 26.46%. The notably deteriorated regions were predominantly patchy and concentrated mainly in Jimei District, the southern part of Tong'an District, and the southwestern part of Xiang'an District. In contrast, the environmental quality within the island (Huli District and Siming District) was well-maintained. (2) From 2010 to 2020, the environmental quality in Xiamen slightly declined, with the area where the environmental quality level decreased amounting to 539.83 km^2, representing 47.03% of the study area . The area where environmental quality worsened accounted for 35.39%, which is 0.53% more than the area where it improved. Most areas outside the island exhibited a slight deterioration, particularly concentrated in the eastern part of Xiang'an District and the northern part of Tong'an District. However, the coastal areas outside the island showed significant improvements in environmental quality, indicating effective ecological management.

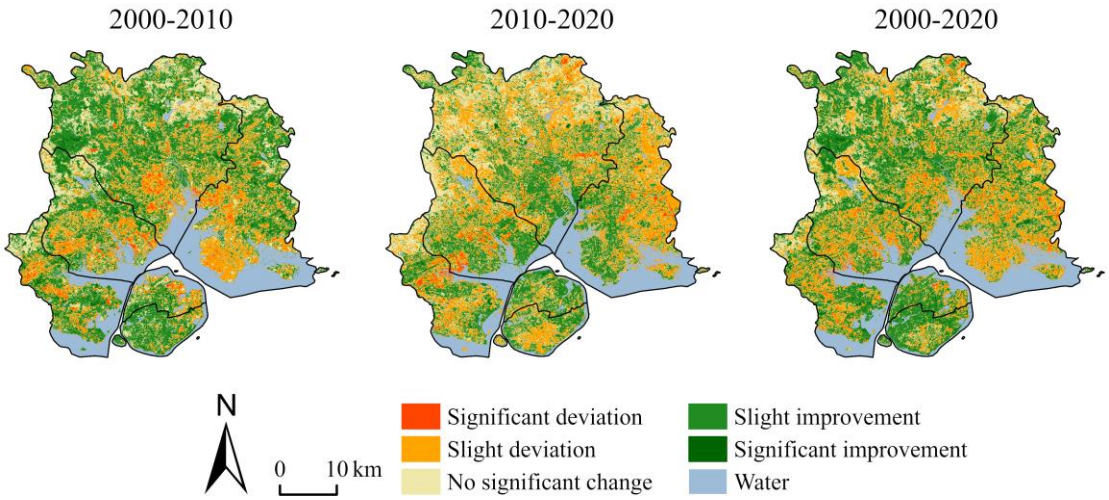

Figure 3. The spatial distribution of changes in the environment quality of Xiamen from 2000 to 2020

Table 5. Changes in the Ecological Grade of Xiamen from 2000 to 2020

RSEI variation category	2000—2010		2010—2020		2000—2020	
	Area (km²)	Scale (%)	Area (km²)	Scale (%)	Area (km²)	Scale (%)
Significant deviation	37.05	2.52%	31.42	2.06%	26.40	1.79%
Slight deviation	352.61	23.95%	508.41	33.33%	454.69	30.79%
No significant change	381.10	25.88%	453.75	29.75%	334.87	22.67%
Slight improvement	668.60	45.41%	519.04	34.03%	626.75	42.44%
Significant improvement	33.13	2.25%	12.72	0.83%	34.12	2.31%

3.3. SHAP feature importance analysis

This study employed the XGBoost model and SHAP method to analyze the mechanisms by which various factors affect the environmental quality of Xiamen, with results shown in Fig. 4. Among them, Fig. 4(a) displays the beesworm distribution of SHAP importance, representing the overall impact of different factors on RSEI. In the figure, labels on the left side are arranged according to the importance of each factor, with the horizontal axis below indicating the SHAP values, which represent the weight of the impact. The wider distribution of the area indicates greater influence of the factor. Each dot represents a sample, and the color indicates the magnitude of the factor's value: redder colors signify higher values, while bluer colors indicate lower values.

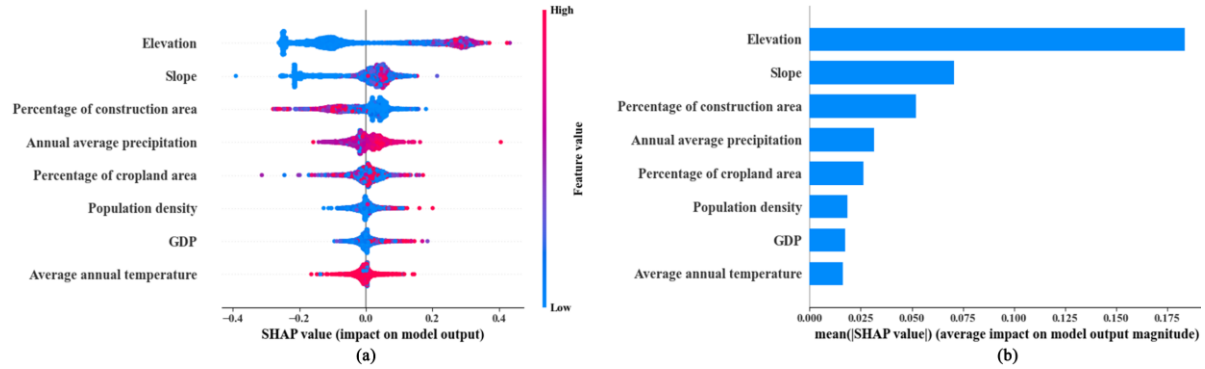

Figure 4. Feature importance ranking based on SHAP value

Overall, elevation, slope, percentage of construction area, annual average precipitation, and percentage of cropland area are the five factors with the greatest impact. Specifically, higher values of elevation and slope have a more positive impact on RSEI, leading to better environmental quality.

Conversely, a higher percentage of construction area has a more negative impact on environmental quality. Additionally, annual average precipitation plays a promotive role in enhancing environmental quality, while the percentage of cropland area has a suppressive effect. Other factors, including GDP, population density, and average annual temperature, do not have a significant impact on RSEI.

3.4. SHAP partial dependence plots analysis

Due to the significant impact of elevation, slope, percentage of construction area, annual average precipitation, and percentage of cropland area on environmental quality, this study selected these five factors for further analysis. The results are shown in Fig. 5, with the specific analysis as follows.

In Fig. 5(a), the relationship between elevation and RSEI appears to be an inverted quadratic function. As elevation increases, its positive impact also grows, reaching a maximum when elevation is around 450 m. Beyond this point, further increases in elevation lead to a reduction in positive impacts and an increase in negative impacts. Similarly, in Fig. 5(b), as slope increases up to 20°, RSEI also increases. This may be because areas at lower elevations and in plains are conducive to the expansion of construction land and socio-economic development, resulting in reduced environmental quality. However, significant increases in elevation and slope may lead to soil erosion, which is detrimental to the growth of most plants, thereby affecting environmental quality. In Fig. 5(d), annual average precipitation generally shows a positive correlation with environmental quality. As this variable increases, RSEI also gradually increases, and the linear relationship is quite apparent. This is because ample precipitation benefits vegetation growth [32], and given that Xiamen has a mild climate with an average annual temperature around 21°C, this results in higher NDVI values, ultimately impacting RSEI.

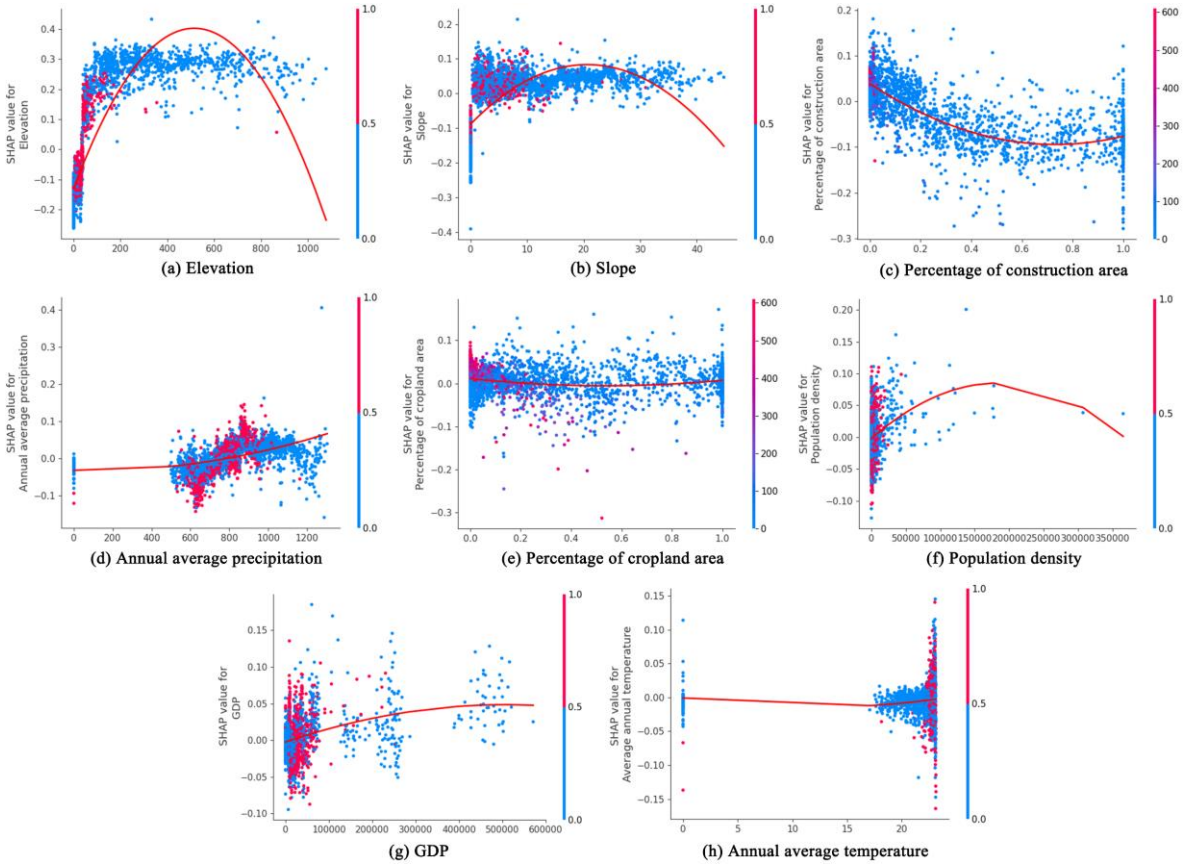

Figure 5. Partial dependence plots analysis

In Fig. 5(c), the impact of the percentage of construction area on environmental quality shows an approximately linear decreasing relationship. This indicates that a larger area occupied by construction sites corresponds to a lower RSEI. Meanwhile, Fig. 5(e) shows that the percentage of cropland area is mainly negatively correlated with RSEI, though the linear relationship is not as

distinct. This is likely because, compared to forest, cropland has a lower diversity of tree species and vegetation cover, leading to a predominantly negative impact of the percentage of cropland area on ecological quality. However, in densely built urban areas, cropland also forms part of the urban green space and provides ecological services. Therefore, an increase in the proportion of cropland within urban built-up areas can enhance NDVI, thereby improving the overall environmental quality.

In summary, while the development of construction land, the increase in cropland area, and frequent human activities can have significant negative impacts on local environmental quality, the rapid urbanization of Xiamen has not led to a notable overall deterioration in environmental quality. This indicates that concurrent development of urbanization and ecological environmental protection is feasible.

4. Conclusion and Discussion

This study, based on the GEE platform, constructs the RSEI model for Xiamen from 2000 to 2020 by coupling four ecological indicators, allowing for long-term monitoring of the city's environmental quality changes over nearly two decades. This extends the application of the GEE platform in evaluating the environmental quality of bay-type cities. Additionally, it integrates the XGBoost model and SHAP method to investigate the factors influencing changes in Xiamen's environmental quality. The main conclusions are as follows: (1) From 2000 to 2020, the environmental quality of Xiamen exhibited a "rise and then fall" trend, with the average RSEI value increasing from 0.55 in 2000 to 0.57 in 2010, and then slightly decreasing to 0.56 in 2020. The environmental grades for each year were predominantly moderate or better, with total area percentages of 69.31%, 67.33%, and 65.14%, respectively, indicating an overall improvement in ecological environmental quality. (2) From the perspective of spatial distribution, between 2000 and 2020, the environmental quality of Xiamen primarily improved, with an area proportion of 44.75%. The ecological environment management in the island areas (Huli District and Siming District) and Tong'an District was particularly effective. Conversely, the areas where the environment deteriorated were mainly distributed along the coastal regions of Jimei District and Xiang'an District, accounting for 32.58% of the total area. (3) The SHAP analysis results indicate that elevation, slope, percentage of construction area, annual average precipitation, and percentage of cropland area are the five factors with the greatest impact on environmental quality. Among these, factors such as elevation, slope, and annual average precipitation have a positive effect on environmental quality, while the percentage of construction area and percentage of cropland area primarily exert inhibitory effects. (4) The mechanisms by which each factor affects environmental quality vary. Elevation and slope impact ecological quality in a manner akin to a quadratic function, while the percentage of construction area, annual average precipitation, and percentage of cropland area influence environmental quality in a linear relationship.

However, to avoid the influence of large water bodies on WET in the study area, the MNDWI was used to mask aquatic information. This means that this study only monitored the environmental quality of the terrestrial areas in Xiamen. Nevertheless, water bodies are an essential component of ecosystems and play a vital role in maintaining biodiversity and regional ecological balance. Therefore, in future research, we will employ more comprehensive and effective evaluation methods to monitor the overall environmental changes in Xiamen, providing more accurate data support for the city's future development planning.

References

[1] Y. Xu, Q. Dai, Y. Lu, C. Zhao, W. Huang, M. Xu, and Y. Feng, "Identification of ecologically sensitive zones affected by climate change and anthropogenic activities in Southwest China through a NDVI-based spatial-temporal model," Ecological Indicators, vol. 158, Art. no. 111482, January 2024.

[2] W. Xu, J. Song, Y. Long, R. Mao, B. Tang, and B. Li, "Analysis and simulation of the driving mechanism and ecological effects of land cover change in the Weihe River basin, China," Journal of Environmental Management, vol. 344, Art. no. 118320, October 2023.

[3] J. C. Jimenez-Munoz, J. Cristobal, J. A. Sobrino, G. Sòria, M. Ninyerola, and X. Pons, "Revision of the single-channel algorithm for land surface temperature retrieval from Landsat thermal-infrared data," IEEE Transactions on geoscience and remote sensing, vol. 47, pp. 339-349, January 2008.

[4] J. Teng, S. Xia, Y. Liu, X. Yu, H. Duan, H. Xiao, and C. Zhao, "Assessing habitat suitability for wintering geese by using Normalized Difference Water Index (NDWI) in a large floodplain wetland, China," Ecological Indicators, vol. 122, Art. no. 107260, March 2021.

[5] H. Yang, J. Yu, W. Xu, Y. Wu, X. Lei, J. Ye, J. Geng, and Z. Ding, "Long-time series ecological environment quality monitoring and cause analysis in the Dianchi Lake Basin, China," Ecological Indicators, vol. 148, Art. no. 110084, April 2023.

[6] S. Li, C. Liu, C. Ge, J. Yang, Z. Liang, X. Li, and X. Cao, "Ecosystem health assessment using PSR model and obstacle factor diagnosis for Haizhou Bay, China," Ocean & Coastal Management, vol. 250, Art. no. 107024, April 2024.

[7] X. Hu, C. Ma, P. Huang, and X. Guo, "Ecological vulnerability assessment based on AHP-PSR method and analysis of its single parameter sensitivity and spatial autocorrelation for ecological protection–A case of Weifang City, China," Ecological Indicators, vol. 125, Art. no. 107464, June 2021.

[8] P. Zhang, H. Xu, Q. Du, H. Ling, P. Zhang, and X. Zhao, "Ecological environment assessment of Tarim River main stream based on RS and GIS," Arid Zone Research, vol. 34, pp. 416-422, April 2017.

[9] Z. Zheng, Z. Wu, Y. Chen, C. Guo, and F. Marinello, "Instability of remote sensing based ecological index (RSEI) and its improvement for time series analysis," Science of the Total Environment, vol. 814, Art. no. 152595, March 2022.

[10] H. Xu, "A remote sensing index for assessment of regional ecological changes," China Environmental Science, vol. 33, pp. 889-897, May 2013.

[11] H. Yang, W. Xu, J. Yu, X. Xie, Z. Xie, X. Lei, Z. Wu, and Z. Ding, "Exploring the impact of changing landscape patterns on ecological quality in different cities: A comparative study among three megacities in eastern and western China," Ecological Informatics, vol. 77, Art. no. 102255, November 2023.

[12] Y. Zhang, J. She, X. Long, and M. Zhang, "Spatio-temporal evolution and driving factors of eco-environmental quality based on RSEI in Chang-Zhu-Tan metropolitan circle, central China," Ecological Indicators, vol. 144, Art. no. 109436, November 2022.

[13] C. Gong, F. Lyu and Y. Wang, "Spatiotemporal change and drivers of ecosystem quality in the Loess Plateau based on RSEI: A case study of Shanxi, China," Ecological Indicators, vol. 155, Art. no. 111060, November 2023.

[14] Z. Cao, M. Wu, D. Wang, B. Wan, H. Jiang, X. Tan, and Q. Zhang, "Space-time cube uncovers spatiotemporal patterns of basin ecological quality and their relationship with water eutrophication," Science of The Total Environment, vol. 916, Art. no.170195, March 2024.

[15] Z. Cai, Z. Zhang, F. Zhao, X. Guo, J. Zhao, Y. Xu, and X. Liu, "Assessment of eco-environmental quality changes and spatial heterogeneity in the Yellow River Delta based on the remote sensing ecological index and geo-detector model," Ecological Informatics, vol. 77, Art. no. 102203, November 2023.

[16] Y. Lv, L. Xiu, X. Yao, Z. Yu, and X. Huang, "Spatiotemporal evolution and driving factors analysis of the eco-quality in the Lanxi urban agglomeration," Ecological Indicators, vol. 156, Art. no. 111114, December 2023.

[17] X. Zhang, W. Jia and J. He, "Spatial and temporal variation of ecological quality in northeastern China and analysis of influencing factors," Journal of Cleaner Production, vol. 423, Art. no. 138650, October 2023.

[18] F. Wang, F. Wang, H. Yang, J. Yu, and R. Ni, "Ecological risk assessment based on soil adsorption capacity for heavy metals in Taihu basin, China," Environmental Pollution, vol. 316, Art. no. 120608, January 2023.

[19] Y. Yang, M. Shi, B. Liu, Y. Yi, J. Wang, and H. Zhao, "Contribution of ecological restoration projects to long-term changes in PM2. 5," Ecological Indicators, vol. 159, Art. no. 111630, February 2024.

[20] X. Ma, J. Zhang, P. Wang, L. Zhou, and Y. Sun, "Estimating the nonlinear response of landscape patterns to ecological resilience using a random forest algorithm: Evidence from the Yangtze River Delta," Ecological Indicators, vol. 153, Art. no. 110409, September 2023.

[21] J. Wan and T. Fei, "Production-Living-Ecological Spaces" Recognition Methods based on Street View Images," Journal of Geo-information Science, vol. 25, pp. 838-851, April 2023.

[22] S. M. Lundberg and S. Lee, "A unified approach to interpreting model predictions," in Proceedings of the 31st International Conference on Neural Information Processing Systems, Long Beach, CA, USA, 2017, pp. 4768-4777.

[23] S. Wang, and H. Peng, " Multiple spatio-temporal scale runoff forecasting and driving mechanism exploration by K-means optimized XGBoost and SHAP," Journal of Hydrology, vol. 630, Art. no. 130650, January 2024.

[24] X. Liu, J. Zeng and P. Zeng, "Construction and Optimization of the Green Space Ecological Network in Xiamen City," Chinese Landscape Architecture, vol. 36, pp. 76-81, July 2020.

[25] J. Yang and X. Huang, "30 m annual land cover and its dynamics in China from 1990 to 2019," Earth System Science Data Discussions, vol. 2021, pp. 1-29, Augest 2021.

[26] C. Song, B. Huang and S. You, "Comparison of three time-series NDVI reconstruction methods based on TIMESAT," in Geoscience and Remote Sensing Symposium (IGARSS), 2012 IEEE International. IEEE, 2012, pp. 2225-2228.

[27] E. P. Crist, "A TM tasseled cap equivalent transformation for reflectance factor data," Remote sensing of Environment, vol. 17, pp. 301-306, June 1985.

[28] H. Xu, "A new index for delineating built-up land features in satellite imagery," International journal of remote sensing, vol. 29, pp. 4269-4276, October 2008.

[29] J. A. Sobrino, J. C. Jiménez-Muñoz and L. Paolini, "Land surface temperature retrieval from LANDSAT TM 5," Remote Sensing of environment, vol. 90, pp. 434-440, April 2004.

[30] S. M. Lundberg, G. Erion, H. Chen, A. DeGrave, J. M. Prutkin, B. Nair, R. Katz, J. Himmelfarb, N. Bansal, and S. Lee, "From local explanations to global understanding with explainable AI for trees," Nature machine intelligence, vol. 2, pp. 56-67, January 2020.

[31] Z. Chen, H. Yang, Y. Lin, J. Xie, Y. Xie, and Z. Ding, "Exploring the association between the built environment and positive sentiments of tourists in traditional villages in Fuzhou, China," Ecological Informatics, vol. 80, Art. no. 102465, May 2024.

[32] A. Mohammat, X. Wang, X. Xu, L. Peng, Y. Yang, X. Zhang, R. B. Myneni, and S. Piao, "Drought and spring cooling induced recent decrease in vegetation growth in Inner Asia," Agricultural and Forest Meteorology, vol. 178, pp. 21-30, September 2013.

[33] B. Yuan, L. Fu, Y. Zou, S. Zhang, X. Chen, F. Li, Z. Deng, and Y. Xie, "Spatiotemporal change detection of ecological quality and the associated affecting factors in Dongting Lake Basin, based on RSEI," Journal of Cleaner Production, vol. 302, Art. no. 126995, June 2021.